LA-UR- 97-4720

CONF-971168--

CHEMISTRY MODIFICATION OF HIGH OXYGEN-CARBON POWDER BY PLASMA MELTING: FOLLOW UP TO COMPLETE THE STORY

P. S. Dunn, D. R. Korzekwa, F. G. Garcia
Los Alamos National Laboratory

C. A. Michaluk
Cabot Performance Materials

ABSTRACT

State-of-the-art melting of tantalum and tantalum alloys has relied on electron beam (EB) or vacuum arc remelting (VAR) for commercial ingot production. Plasma arc melting (PAM) provides an alternative for melting tantalum that contains very high levels of interstitials where other melting techniques can not be applied. Previous work in this area centered on plasma arc melt quality and final interstitial content of tantalum feedstock containing excessive levels of interstitial impurities as a function of melt rate and plasma gas.(1) This report is an expansion of this prior study and provides the findings from the analysis of second-phase components observed in the microstructure of the PAM tantalum. In addition, results from subsequent EB melting trials of PAM tantalum are included.

INTRODUCTION

Because of the high melting point and reactivity of tantalum, production of mill forms rely on EB or EB+VAR melting to achieve purity levels greater than 99.95%. High vacuum levels inherent in EB melting, combined with the high melting point of tantalum, acts to purify the product by volatilizing interstitial and low melting metallic impurities(2). High-quality Ta products exhibiting consistent mechanical and metallurgical properties are produced from large diameter (300mm) ingots which were triple EB melted(3). Here, tantalum powder billets are side fed into the furnace and melted into an ingot which is then inverted and hung in the furnace and remelted; this process is repeated to produce a 3EB ingot. The purpose of the first EB melt is to consolidate the powder into a homogeneous form; purification is achieved primarilly from the final two EB melts. An alternative to the 3EB process involves double EB melting of a tantalum electrode followed by a final VAR melt. The VAR process affords a greater melt rate, and operates at a vacuum pressure which is 2-3 orders of magnitute higher than EB melting. Tantalum plate stock produced from 2EB+VAR ingots has been characterized as having a finer grain size and a greater strength compared to 3EB products. Early speculation was that the difference in properties between 3EB and 2EB+VAR tantalum products was due to the finer grain size of the VAR ingot; however, recent studies indicate that these differences are a reflection of product purity.(3,4)

DISCLAIMER

As with any technique, the EB and VAR processes have limits on the form and purity of material that can be processed. For instance, the VAR process requires structural integrity and electrical conductivity of the starting material. In addition, the fabricated electrode must be of similar cross section over its length if the arc is to be controlled. The EB process requires a constant vacuum for the electron guns to function which limits the amount of outgassing that can occur during melting. However, material form is not a concern due to the side feed design of most EB systems.

The plasma arc melting (PAM) process offers the advantages of both EB and VAR. As with EB, starting material is side fed so that starting feed form is not a concern. However, the PAM process operates under inert atmospheres and a wide pressure range, so that outgassing of feed material does not disrupt the melting process. The gas from the melt is simply swept out of the melt chamber. The plasma melt process also allows flexibility in plasma gas composition which relates to significant changes in melt quality(5-7)and chemistry during melting(8,9). For example, the plasma process allows melt chemistry modification by injecting various gas elements (hydrogen, oxygen, carbon dioxide or nitrogen) into the cover gas which react with the melt to reduce oxides or remove carbon through the formation of carbon monoxide(10,11).

Thermodynamic modeling provides insight on the purification processes which occur during EB melting of tantalum. For tantalum liquid at 3273°K, oxygen is contained in three phases: Ta_2O_5 (liquid), TaO_2 (gas), and TaO (gas). The relative amounts of each oxide in equilibrium is dependent on pressure: as vacuum levels increase, the amount of Ta_2O_5 decreases while the concentration of suboxides increases. During EB melting of high-purity tantalum powder in the absence of other reducing agents, oxygen is removed primarilly as TaO. However, when carbon is present, CO is the energitically favorable reduction product. When carbon content is stochiometrically less than oxygen, the CO reaction will deplete the carbon, and excess oxygen would be reduced as TaO. Should the opposite condition exist, excess carbon will remain in the tantalum as TaC. Hydrogen is incapable of reducing oxygen in tantalum, owed to the stability of tantalum oxide and suboxides, and nitrogen can only be removed as N_2.

Tantalum containing excessive amounts of oxygen poses difficulties with EB melting. First, rapid outgassing during melting can cause the melt pool to splatter tantalum throughout the furnace, and can create pressure spikes which shut-down the guns. Also, since oxygen is removed as TaO, yield losses associated with melting high-oxygen tantalum can make the process economically prohibitive.

Previous work by Minura and Nanjo(12) has demonstrated that tantalum oxide can be reduced with plasma as the heat source by the carbothermal reduction process. The purpose of the current work was to; 1) evaluate the plasma melting process for the recycle of very low grade tantalum powder containing excessive levels of interstitials, 2) determine the effect of argon-hydrogen and helium-hydrogen plasma gas mixtures on melt quality and final interstitial content, and 3) establish a processing window to determine the parameters of plasma cover gas and melt rates that might be used in commercial applications.

EXPERIMENTAL APPROACH

Starting Material

The starting material for this investigation was obtained from Cabot Corporation. The material consisted of low-grade high-interstitial scrap powder. Mixed with the powder was other tantalum material with interstitial levels greater than the matrix composition. Figure 1 shows a cross section of the sintered logs. The light phase in the cross section is the very high interstitial material.

The blended composite mixture was pressed into billets then vacuum sintered. Attempts to electron beam melt the material were unsuccessful because outgassing significantly reduced beam intensity to the point of actual gun shutdown. The chemical composition of the starting tantalum is given in Table I.

Figure 1. Macrograph of the starting material for this investigation. Note the light phase material which is very high interstitial content tantalum.

Table I. Chemical Composition (ppm wt. %) of Tantalum Powder

Element	O	C	H
Composition(wt ppm)	10700	15810	6

Melting Parameters: Plasma Melting

Melt parameters were established based on viable commercial applications for the recycling of the tantalum powder. Melt rates were held to within an order of magnitude of conventional EB processing. Plasma gas selection was limited to compositions that could be easily handled in an industrial application and not pose major safety concerns. Power input, voltage and current, and torch profile parameters; standoff and articulation were held constant. A total of six plasma gas compositions were examined. Table II is a compilation of all melting and torch parameters.

Table II. Melting and Torch Parameters Used in The Current Investigation

Melt Rates: 2.6 grams/s and 5.2 grams/s into a 100 mm dia ingot.
Gas Compositions: He, He-3% H_2, He-6% H_2, Ar, Ar-3% H_2, Ar-6% H_2
Power Input: Constant 150-165 V, 540-510 amps
Torch Profile: Constant standoff / Constant torch profile

Melt Parameters: Electron Beam

Plasma consolidated tantalum, in the form of pucks appoximately 100mm in diameter and 50mm thick, were side fed and EB melted in Cabot Performance Materials' 1200KW, 6-gun Lehybold Electron Beam Furnace. Two guns were focussed to melt the pucks, while the remaining 4 guns were concentrated on heating the melt pool. Feedstock was melted onto a preheated starting block, and produced a casting which was 250mm in daimeter and approximately 75mm long. Power input and

vacuum levels in the EB furnace were maintained with the plasma melted material, which was in sharp contrast to previous attempts in EB melting the starting material.

RESULTS

Melt Quality: Plasma Melting

Melt quality was determined based on observations of material spatter, depth of melt pool and melt pool geometry. Table III is a compilation of observations made during melting with various plasma gasses. In general, melt quality using any of the helium gas compositions was superior to that when argon gas was used. Pure argon gas resulted in only localized melting with no true defined melt pool.

Table III. Observations of Melt Quality During Melting of Tantalum Powder

Gas Composition	Observation
Ar	Poor melt quality. Only localized melting with considerable spatter.
Ar-3H_2	Beginning of coherent melt pool. Material continues to spatter.
Ar-6H_2	Well defined melt pool approximately 2 cm depth. Minimal spatter.
He	Good plasma control. Good melt pool; 3 cm depth. No spatter.
He-3H_2	Same as pure He but increased melt pool area and depth.
He-6H_2	Excellent pool geometry. No spatter. Pool depth approximately 5 cm.

Qualitative differences in the melting can be seen in Figure 2 with a comparison of pure argon and helium plasma gasses.

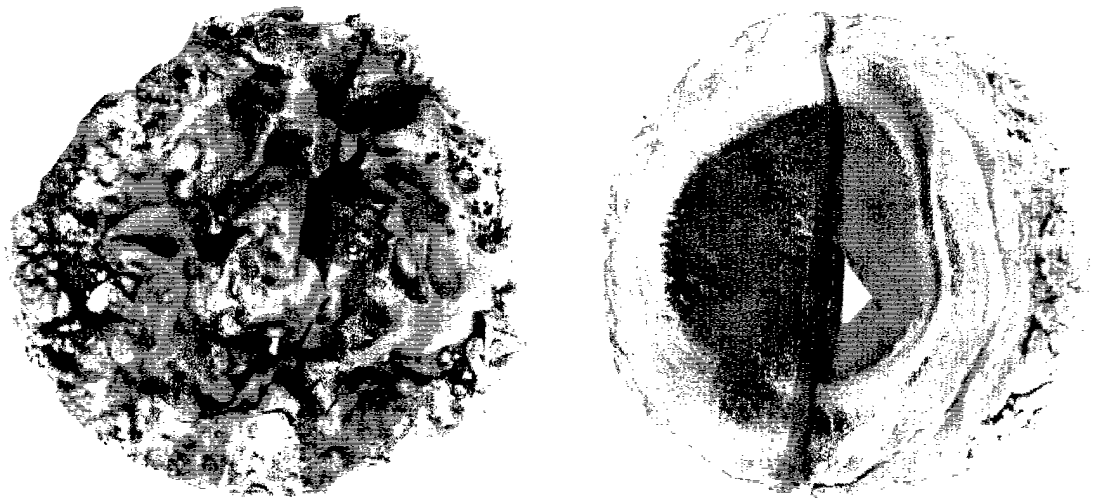

Argon Plasma Gas **Helium Plasma Gas**

Figure 2 Macrograph of melted tantalum ingots using argon and helium plasma gasses.

Both ingots in the figure were melted at 2.6 grams/sec. The helium ingot shows a well established melt pool and smooth surface. The argon ingot never established a coherent melt pool and resulted in

extensive spatter. The melt quality with the pure argon gas and fast melt rate, 5.2 grams/s, resulted in only a partially melted slug and extensive splatter during melting. Since the starting material could not be completely melted, no further analysis was performed on this material.

Ingot Chemistry: Plasma melting

Each of the melted ingots was analyzed for final interstitial contents of carbon, oxygen and hydrogen. A concern before running the experiments was the possible pickup of hydrogen from the plasma gas, therefore the analysis included this element. Comparisons were then made for interstitial removal as a function of plasma gas composition and melt rate. Figure 3 is a plot of remaining interstitial content for various plasma gasses. All data are for the lower melt rate of 2.6 grams/s. The interstitial content of the starting material is plotted for comparison.

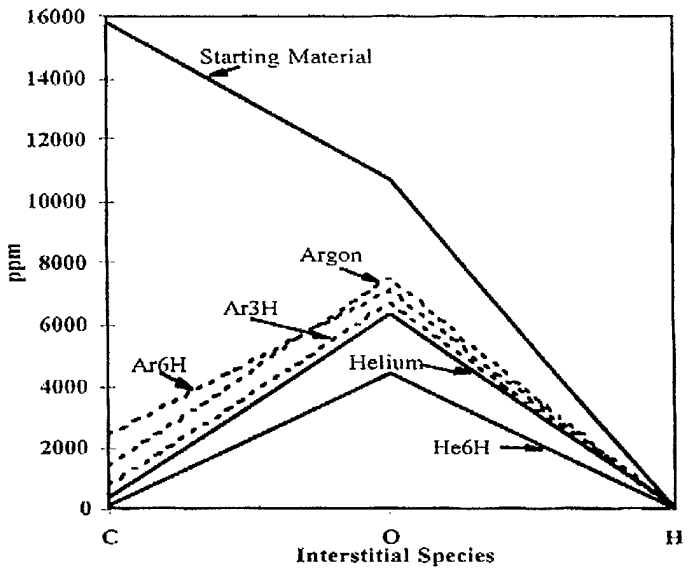

Figure 3. Interstitial content of the tantalum ingots as a function of plasma gas.

If all the initially retained carbon reacted with oxygen to form CO, the final tantalum oxygen concentration would be approximately 1600 ppm. Since the final interstitial compositions for all samples were above this level, not all of the carbon reacted. There are two possible explanations for the final chemistries. First, the melt rates were too fast to allow for the complete reaction. The work by Minura et.al. (9) would support this hypothesis. In that work, melt rates were less than 1 gram/minute to achieve complete reaction. The second possibility is the inhomogeneity of the starting material. The higher interstitial content light phase seen in Figure 1 could easily skew the results depending on the phase distribution within the log.

In spite of the variations in compositions, the plots in Figure 3 reveal that the helium gasses are more effective in removing the interstitials compared to the argon series. These results are the same as the melt quality analysis and indicate that the higher heat content and thermal conductivity of the helium series gases are resulting in a hotter melt pool. Furthermore, the plots in Figure 3 follow the general trend of lower interstitial content with increased hydrogen content in the cover gas. This observation is in constrast to the predictions based on thermodynamic analysis. The model determined the equilibrium concentration of species based on thermodynamic data of elemental and molecular constituents; data from ionic species were not included in the data files, thus they were not included in the thermodynamic analysis. It is speculated that a fraction of the hydrogen present in the plasma existed as H^+, and the ionic hydrogen contributed to the reduction of oxygen and carbon during plasma melting.

The hotter melt pool has three thermodynamic benefits for removing the carbon and oxygen. The higher melt pool temperature will thermodynamically enhance the formation of CO. An increase in temperature for this reaction results in an increase in the free energy of formation and will tend to drive the reaction further to completion. As the melt temperature increases, the tantalum oxide heat of formation will decrease making the oxide less stable. The reduction in free energy will allow further direct dissociation of the oxide compared to a lower temperature system. Finally, the ionic hydrogen in the plasma gas will contribute to lowering the oxygen content by direct reduction. The hydrogen content in the final ingots remained low in spite of the relatively large amount of the gas introduced into the system. The compositions varied from 20 to 70 ppm hydrogen with no correlation to hydrogen content in the gas. Table IV shows the compilation of final interstitial chemistries for the 2.6 gram/s melt rate and six plasma gasses.

Table IV. Final Interstitial Content For The Low Melt Rate Tantalum Ingots

Plasma Gas	O	C	H	N
Ar	7541	1427	66	7622
Ar-3H_2	6724	758	57	5787
Ar-6H_2	7123	2466	23	2189
He	6334	371	146	3839
He-3H_2	6506	984	56	2689
He-6H_2	4403	130	26	1513

Ingot Chemistry: EB Melting

After the final EB melting, chemistry samples were taken from three locations on the 250 mm diameter ingot; side wall edge, top edge and top middle. Table V shows the interstital chemistries for the e-beam melted ingot.

Table V. Final Interstital Content For the Electron Beam Melted Tantalum Ingot

Location	O	C	H	N
Side Wall	<10	<4	<5	86
Top Edge	<10	<5	<5	59
Top Middle	59	<5	<5	98

The final chemistries were very good considering the relatively high values from the plasma melted material. Nitrogen was the only interstitial that remained high after EB melting, which was anticipated based on thermodynamic analysis and previous melting experience. Whereas EB melting removes oxygen through the formation of gaseous sub-oxides, nitrogen is removed as N2. Nitrogen reduction is limited by the diffusion of N atoms to the surface of the melt, and the probability of there being a neighboring nitrogen atom available with to bond.

Ingot Image Anaysis: Optical, X-ray and Auger

Optical metallography, X-ray diffraction and Auger analysis was used to characterize all of the plasma melted ingots with an interest in confirming the chemistry results and determining the change

in second-phase morphology with varying interstitial content. Figure 4 shows the change in second phase with variations in carbon and oxygen content. Figure 4 C and 4 D are the same ingot but at two different magnifications; 100X and 250X

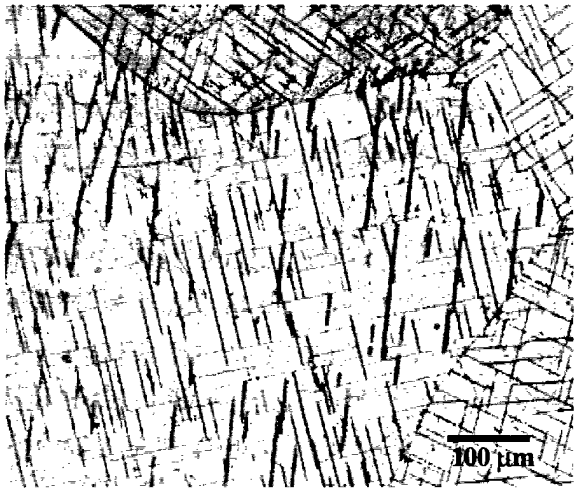

A. Low Carbon and Oxygen

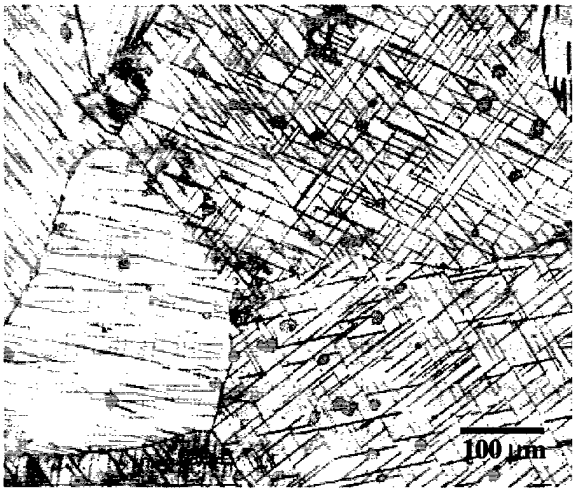

B. Low Carbon and High Oxygen

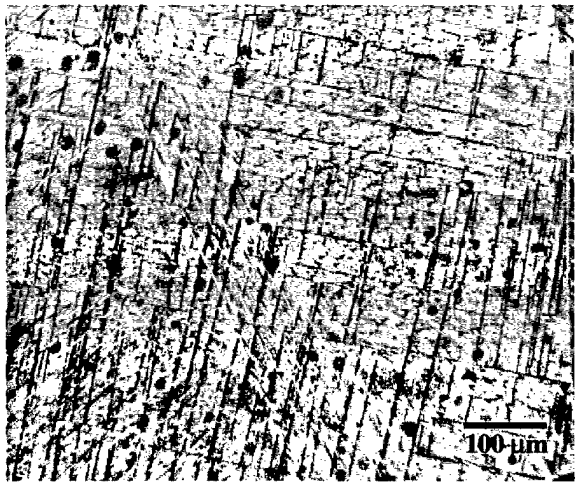

C. High Carbon and High Oxygen

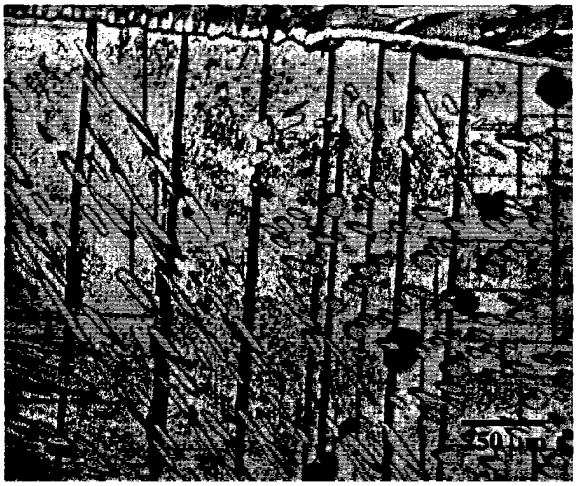

D. High Carbon and High Oxygen; High Mag.

Figure 4: Variation in second phase particles with increasing oxygen and carbon content.

As oxygen content increases, the gray round second phase becomes more pronounced in the microstructure as seen when comparing Figures 4 A and B. As the carbon level increases with increased oxygen, a white lenticular phase begins to appear within the grains as well as decorating the grain boundries, Figure 4 C. Figure 4 D is a higher magnification micrograph of 4 C.

X-ray diffraction was used to confirm the change in second phase. Figure 5 shows the microstructure and corresponding x-ray analysis for the ingot melted under Ar-6H plasma gas. The diffraction pattern in Figure 5 confirms the presence of tantalum oxide as well as lines for tantalum carbide. Also shown is the nitrogen pickup during melting.

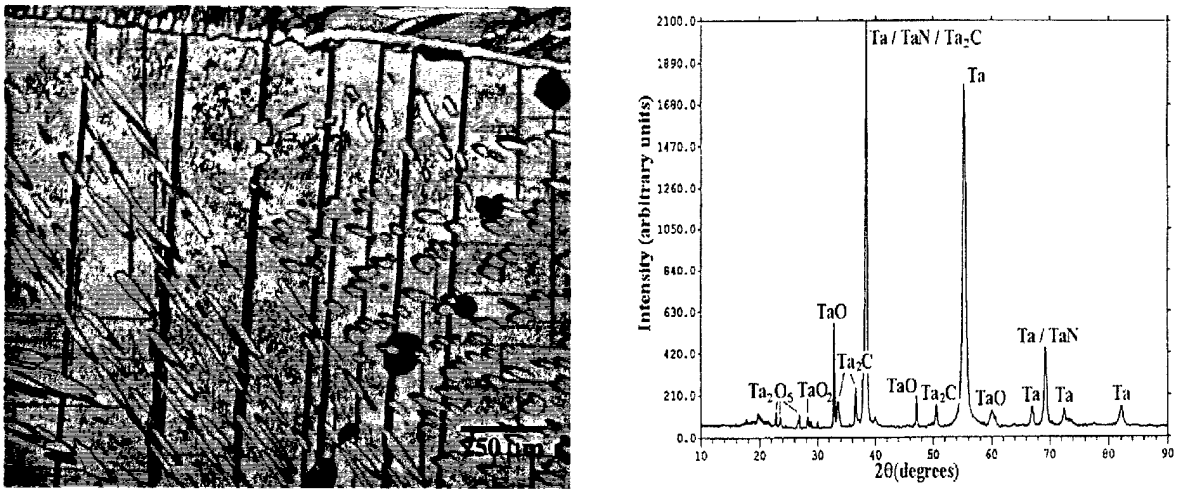

Figure 5. Micrograph and X-Ray diffraction lines for the tantalum ingot with high oxygen and carbon content.

Figure 6 shows the same comparison for the ingot melted under He-6H plasma gas and corresponds to the cleaner microstructure and lower interstitial content. The diffraction pattern for this sample shows only tantalum and possibly a very low tantalum oxide, Ta_6O and the tantalum nitride.

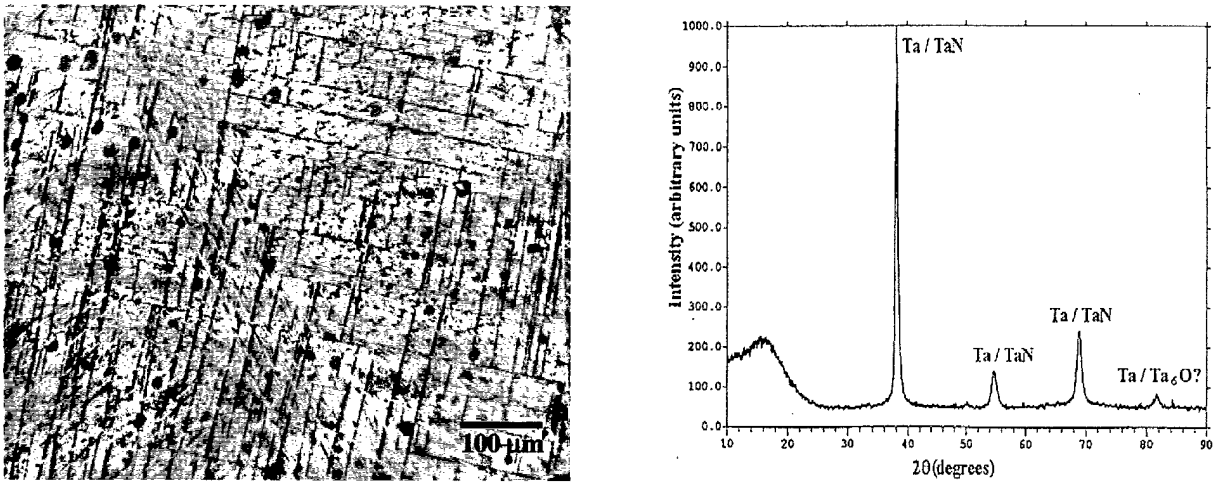

Figure 6. Micrograph and X-Ray diffraction lines for the tantalum ingot with low oxygen and carbon content.

Auger analysis was used in an attempt to identify the second phase particles. Figure 7 shows dot maps for carbon and oxygen analysis of the gray round second phase. The analysis confirms that this phase is tantalum oxide. However, analysis of the other second phase morphologies was not successful in determining composition.

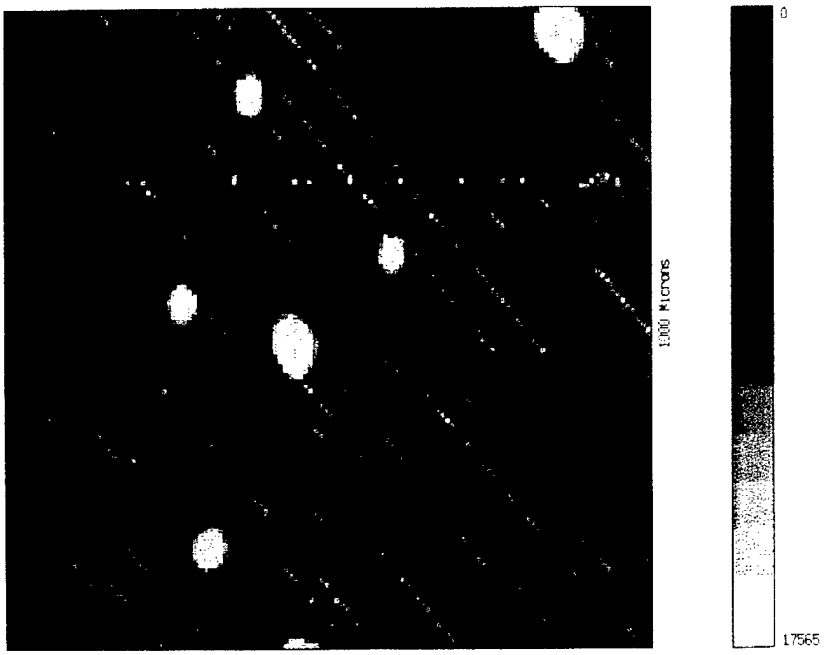

Figure7. Auger dot map scan for oxygen in spherodized tantalum second phase.

CONCLUSIONS

The current work indicates that plasma melting offers a viable processing approach for the recycling of high-interstitial contaminated tantalum powder. While the interstitial levels in the melted ingots were still high, the plasma melting lowered the oxygen and carbon to a level acceptable for subsequent electron beam melting. Based on the parameters in this study:

a) Plasma arc melting is the only alternative for melting high interstitial content material due to excessive outgassing.

b) Pure argon is the least efficient plasma gas based on melt quality or interstitial removal. Compositions of argon-hydrogen are acceptable but at lower melt rates considered in this work.

c) He-6% H plasma gas produced the best melting results and the greatest reduction in interstitial content at the 2.6 gram/s melt rate.

d) Hydrogen uptake in the tantalum ingot, due to additions to the plasma gas, is minimal.

e) Additional purification is realized by EB melting the plasma consolidated material.

Acknowledgments

The authors wish to acknowledge Ann Kelly for the excellent metallographic preparation and Julie Bremser for the X-Ray diffraction analysis. This work was conducted under the auspices of the U.S. Department of Energy.

Refereces

1. P.S. Dunn, D.R. Korzekwa and F.D. Garcia, "Chemistry Modification of High Oxygen-Carbon Powder By Plasma Melting", *Tantalum,* Proceedings of a Symposium, 125 TMS Annual Meeting, edited by E. Chen etal., TMS, Warrendale, PA, 1996, p 325.

2. M.L. Pochon, Columbium and Tantalum (eds. R.T. Sisco and E. Epremian, New York, NY: John Wiley & Sons, Inc. 1963), 176.

3. C.A. Michaluk, "Factors Affecting the Mechanical Properties and Texture of Tantalum", *Tantalum,* Proceedings of a Symposium, 125 TMS Annual Meeting, edited by E. Chen etal., TMS, Warrendale, PA, 1996, pg 325

4. C.A. Michaluk and D.C. Hughes, "Characterization of Ballistic Grade Tantalum Produced by 2EB, 2EB+VAR, and 3EB Melting", Cabot Performance Materials, Master File Report 789.

5. R.M. Gage, "The Principles of the Modern Arc Torch", Welding Journal, 10 (1959), 18.

6. K. Hanusch and H. Winterhager, ".An Alternative for Metallurgical Applications Using the Plasma Torch" Metall. 24 (10) (1970), 1061.

7. F.K. Mc Taggert, Plasma Chemistry in Electrical Discharges (New York, NY: American Elsevier Publishing Company, 1967), 329.

8. V. Dembovsky, Plasma Metallurgy: The Principles (New York, NY: Elsevier Publishing Company, 1985), 262.

9. C.V. Robino, "Representation of Mixed Gases on Free Energy Diagrams," Metall. Matls. Trans. B, 27B (1996) 65-69.

10. F.D. Richardson, " The Thermodynamics of Metallurgical Carbides and Carbon in Steel", Journal of Iron and Steel Institute, 175 (1953) 33-51.

11. D.R. Milner, " Survey of Scientific Principles Related to Wetting and Spreading" British Welding Journal, 5 (3) 1958, 90-105.

12. K. Mimura and N. Nanjo, "Production of Pure Tantalum By Carbon-Reduction Smelting and Hydrogen Plasma-Arc Melting with Refining," Met. Trans., JIM, 31 (10) (1990), 293-301.

Report Number (14) LA-UR--97-4720
CONF-971168--

Publ. Date (11) 199803
Sponsor Code (18) DOE/DP, XF
UC Category (19) UC-701, DOE/ER

DOE